Published in final edited form as:
Int Immunol. 2008 July ; 20(7): 811–818. doi:10.1093/intimm/dxn039.

Bam32: a novel mediator of Erk activation in T cells

Connie L. Sommers[1], **Jordan M. Gurson**[1], **Rishi Surana**[1], **Mira Barda-Saad**[1], **Jan Lee**[2], **Aparna Kishor**[1], **WenMei Li**[1], **Adam J. Gasser**[1], **Valarie A. Barr**[1], **Michihiko Miyaji**[1], **Paul E. Love**[3], and **Lawrence E. Samelson**[1]

1*Laboratory of Cellular and Molecular Biology, National Cancer Institute, National Institutes of Health, Bethesda, MD 20892, USA*

2*Division of Therapeutic Proteins, Center for Biologics Evaluation and Research, Food and Drug Administration, Bethesda, MD 20892, USA*

3*Laboratory of Mammalian Genes and Development, National Institute of Child Health and Human Development, National Institutes of Health, Bethesda, MD 20892, USA*

Abstract

Bam32 (B lymphocyte adapter molecule of 32 kDa) is an adapter protein expressed in some hematopoietic cells including B and T lymphocytes. It was previously shown that Bam32-deficient mice have defects in various aspects of B cell activation including B cell receptor (BCR)-induced Erk activation, BCR-induced proliferation and T-independent antibody responses. In this study, we have examined the role of Bam32 in T cell activation using Bam32-deficient mice. By comparing $CD4^+$ T cells from lymph nodes of wild-type and Bam32-deficient mice, we found that Bam32 was required for optimal TCR-induced Erk activation, cytokine production, proliferation and actin-mediated spreading of $CD4^+$ T cells. These results indicate a novel pathway to Erk activation in T cells involving the adapter protein Bam32.

Keywords

Erk; IL-4; proliferation; TCR; T lymphocyte

Introduction

Bam32 (B lymphocyte adapter molecule of 32 kDa), also known as DAPP1 and PHISH, is an SH2 and pleckstrin homology (PH) domain-containing adapter molecule expressed in B cells, T cells, dendritic cells and macrophages (1,2). Bam32 is found at the cell membrane and has high affinity for lipid products in the phosphoinositide-3 kinase (PI3K) pathway, specifically phosphatidylinositol(3,4,5)P_3 and phosphatidylinositol(3,4)P_2 (3–5). Bam32 also contains a tyrosine in the intervening region between its SH2 and PH domains. This tyrosine can be phosphorylated in response to activation through the B cell receptor (BCR) and this phosphorylation is critical for downstream signaling from the BCR (6,7). In B cells, Bam32 has been reported to co-immunoprecipitate with HPK-1 (2) and PLC-γ2 (6). Generation of Bam32-null mice has helped demonstrate the involvement of Bam32 in B cell activation. In Bam32 null mice, B cell development is unaffected. However, Bam32-deficient B cells have partial defects in Erk and Jnk activation and in anti-IgM-mediated proliferation (2). In addition, Bam32 has been shown to be involved in actin remodeling and BCR internalization in B cell

Correspondence to: L. E. Samelson; E-mail: E-mail: samelson@helix.nih.gov.

lines (7,8). Bam32-deficient mice also have diminished T-independent antibody responses *in vivo* (2,9). Thus, Bam32 appears to optimize B cell activation.

Many signaling pathways coupled to the TCR (T cell antigen receptor) are similar to those activated by BCR engagement. For both receptors, Src and Syk family kinases are activated upon receptor cross-linking, leading to the rapid tyrosine phosphorylation of adapters and recruitment and activation of critical enzymes. In T cells, LAT, a transmembrane adapter protein, is rapidly tyrosine phosphorylated following TCR activation. LAT phosphotyrosine residues serve as docking sites for such signaling proteins as PLC-γ1, Gads, Grb2 and PI3K among others (10). Signal transduction through LAT leads to calcium influx and activation of mitogen-activated protein kinase (MAPKs) in T cells (11).

The Erk MAPK can be activated in T cells downstream from LAT by at least two mechanisms. PLC-γ1 binding to phosphorylated LAT results in its activation, which produces inositol (1, 4,5) tris-phosphate (IP3) and diacylglycerol (DAG) from phosphatidylinositol(4,5)P_2. IP3 generation results in release of Ca^{++} from intracellular stores whereas concomitant DAG generation results in activation of the Ras guanine exchange factor (RasGEF or Ras activator) RasGRP. Ras can also be activated subsequent to binding of the adapter protein Grb2 to phosphorylated LAT. In addition to binding LAT, Grb2 binds the RasGEF Son of sevenless (Sos) protein resulting in Ras activation. Adding complexity to these interactions, Ras and RasGEF localization can also modulate Ras activation (12). Downstream from Ras, Erk is activated via activation of Raf and MEK kinases (13). In an effort to discover other molecules that might mediate Erk activation in T cells, and in light of its connection to Erk activation in B cells, we decided to investigate the role of the adapter protein Bam32 in T cells. Using Bam32-deficient mice, we found that Bam32 is important for proliferation and cytokine production in T cells, as well as for the optimal activation of Erk.

Methods

Mice

Bam32 mice were kindly provided by Dr Michel Nussenzweig (Rockefeller University) (2).

Bam32 reverse transcription–PCR

Human peripheral blood lymphocytes were cultured for 2 weeks in media containing 10 ng ml^{-1} IL-2. Cells were then sorted using a FACS Vantage SE with DiVa option (BD Biosciences) to obtain $CD4^+$ ($CD19^-CD3^+CD4^+CD8^-$) and $CD8^+$ ($CD19^-CD3^+CD4^-CD8^+$) T cells. RNA was isolated using Trizol (Invitrogen). cDNA was synthesized using the SuperScript cDNA synthesis system (Invitrogen). Reverse transcription (RT)–PCR was performed using the following primers: forward Bam32, CTCTTCTCCTCTCAAATGGATG and reverse Bam32, CGCTTCCAATCAAAGGCTG; forward GAPDH, TGTGAACCATGAGAAGTATGAC and reverse GAPDH, ATGATGTTCTGGAGAGCCC.

$CD4^+$ T cell purification

$CD4^+$ T cells were purified from lymph node single-cell suspensions using a mouse $CD4^+$ T cell isolation kit and LS MACS separation columns (Miltenyi Biotec) according to the manufacturer's specifications. Cell purity was monitored by flow cytometry using a FACSCalibur (BD Biosciences) and FlowJo analysis software (Tree Star, Inc.).

Proliferation and cytokine assays

Purified cells were plated at 1×10^5 cells per 96 well in RPMI 1640 containing 10% heat-inactivated fetal bovine serum, 2 mM glutamine, 1 mM sodium pyruvate, 1× non-essential amino acids, 5.5×10^{-5} M β-mercaptoethanol, 100 U ml^{-1} penicillin and 100 μg ml^{-1}

streptomycin onto wells pre-coated with anti-CD3ϵ and anti-CD28 (BD Biosciences). After 48 h incubation, aliquots of supernatants were removed for cytokine analysis by SearchLight sample testing service (ThermoFisher Scientific). SearchLight protein arrays are plate-based protein arrays incorporating ELISA and piezoelectric printing technologies. ^{3}H-thymidine was added to cells for 16 additional hours and ^{3}H-thymidine incorporation was quantitated using a Tomtec harvester 96 and scintillation counting. Data are presented as mean ± SD of individual triplicate wells (^{3}H-thymidine incorporation) or as concentration of cytokine for combined triplicate wells from the same experiment.

Calcium flux analysis

Lymph node single-cell suspensions were loaded with indo-1 (Molecular Probes) in HBSS (Biosource) containing 1% heat-inactivated fetal bovine serum, 10 mM HEPES and pluronic (Molecular Probes) (14). Cells were also surface stained with CD4–PE and CD8–FITC (BD Biosciences). At 30 s, biotinylated anti-CD3ϵ (0.5 μg ml^{-1}) and biotinylated anti-CD4 (10 μg ml^{-1}) were added and at 60 s, streptavidin (80 μg ml^{-1}) was added. Calcium flux (ratio of indo-violet to indo-blue) was monitored over 6 min using an LSR II (BD Biosciences). Data were analyzed using FlowJo software.

TCR stimulation and western blotting

CD4^{+} T cells were purified from lymph node single-cell suspensions as described above. Cells were plated onto six wells pre-coated with anti-CD3ϵ at 2.5 μg ml^{-1} (for Erk and Jnk experiments). For p38 analysis, CD4^{+} lymph node T cells were rested at 37°C overnight and were stimulated in wells pre-coated with 5 μg ml^{-1} anti-CD3ϵ and 5 μg ml^{-1} anti-CD28. At the appropriate time points, cells were lysed directly in SDS sample buffer containing β-mercaptoethanol and were sonicated. For gel electrophoresis, 10% Criterion gels were used (Bio-Rad). For Erk western blotting, phospho-p44/42 MAPK (Thr202/Tyr204) (E10) and p44/42 MAPK antibodies were used (Cell Signaling Technology) as well as SuperSignal West Femto Maximum Sensitivity Substrate (Pierce) for ECL detection. For Jnk western blotting, phospho-SAP/JNK (Thr183/Tyr185) and JNK2 (D-2) antibodies were used (Cell Signaling Technology) with Odyssey system detection (LI-COR). For p38 western blotting, phospho-p38 (Thr180/Tyr182) and p38 MAPK antibodies were used (Cell Signaling Technology).

Flow cytometry

Total lymph node cells were stimulated by incubation with biotinylated anti-CD3ε (10 μg ml^{-1}) and anti-CD4 (2.5 μg ml^{-1}) on ice for 30 min followed by cross-linking with streptavidin (20 μg ml^{-1} at 37°C for times indicated). Phorbol myristate acetate stimulation was at 50 ng ml^{-1} for 15 min. Stimulation was stopped using fixation (2% formalin at 37°C for 10 min) and permeabilization (90% methanol on ice for 30 min). Cells were stained with antibodies to CD4 and anti-phospho-Erk (cell signaling technology E10 antibody mentioned above directly conjugated to Alexa Fluor 488). Histograms are shown for gated CD4^{+} lymph node T cells.

Microscopy

CD4^{+} T cells were purified from lymph node single-cell suspensions as described above. Purified T cells were suspended in imaging buffer (RPMI 1640 without phenol red, with 10% heat-inactivated fetal bovine serum and 20 mM HEPES) and dropped onto chamber surfaces pre-coated with anti-CD3ϵ (10 lg ml^{-1}) and anti-CD28 (10 μg ml^{-1}). After 15 min, cells were fixed and stained with phalloidin (Molecular Probes) and anti-phospho-ZAP-70 (Cell Signaling Technology) as previously described (15). Interference reflection microscopic (IRM) and fluorescent images were acquired on a LSM 510 confocal system (Carl Zeiss) using a 63× Plan-Apochromat objective. The images were composed into figures with Adobe Photoshop

(Adobe Systems Inc.). The area and radial standard deviation of spread cells were obtained using IPLab software (Scanalytics Inc.) to analyze the IRM images.

TCR down-modulation

Lymph node cells were harvested and stimulated in wells pre-coated with anti-CD3ϵ (5 μg ml^{-1}). After stimulation, cells were stained with anti-TCRβ and anti-CD4 and analyzed by flow cytometry to determine cell surface levels of TCRβ on $CD4^+$ (gated) T cells. Surface TCRβ levels were quantitated by mean fluorescence intensity (MFI). Percentage TCR down-modulation (at time *t*) was calculated as 100 × (MFI of TCRβ on unstimulated $CD4^+$ T cells at time *t* − MFI of TCRβ on stimulated $CD4^+$ T cells at time *t*)/MFI of TCRβ on unstimulated $CD4^+$ T cells at time 0.

Results

Bam32 expression has been detected in mouse thymic and splenic T cells, albeit at a lower (mRNA) level than in splenic B cells (2). Since Bam32 expression was not previously detected in human T cell lines (6), we wanted to investigate further the expression of Bam32 in human peripheral blood T cells before pursuing a more extensive analysis of the role of Bam32 in T cell signaling. As shown in the RT–PCR experiment in Fig. 1, Bam32 expression was readily detected in sorted human $CD4^+$ and $CD8^+$ peripheral blood T cells as well as in the human Burkitt's lymphoma Daudi cell line. We also detected very weak expression of Bam32 mRNA in Jurkat human leukemic T cells.

Based on our demonstration of Bam32 mRNA expression in human T cells and previous demonstrations of Bam32 expression in mouse T cells, we examined Bam32 knockout mice that had previously been studied for signaling defects in B cells for the purpose of determining the effect of the Bam32 null mutation on T cell development and function (2). Thymic development was normal in Bam32 knockout mice and numbers of mature $CD4^+$ and $CD8^+$ lymph node T cells was also within the normal range (data not shown). Thymic-positive selection was analyzed in Bam32 knockout mice by crossing to HY and DO11.10 TCR transgenic mice as described previously (16,17) and was found to be normal (data not shown). Negative selection was also normal in the presence of the Bam32 null mutation as measured in HY TCR transgenic male mice (data not shown).

We next examined the functional abilities of mature $CD4^+$ lymph node T cells by measuring proliferation and cytokine production in response to *in vitro* TCR cross-linking. Purified T cells were stimulated with plate-bound anti-CD3 (which stimulates TCR), anti-CD28 (which activates CD28, a co-receptor for the TCR) or both anti-CD3 and anti-CD28. As shown in Fig. 2, there was a partial defect in the proliferation of $CD4^+$ lymph node T cells especially in response to inter-mediate levels of TCR stimulation. This was consistent with the previously described effect of the Bam32 null mutation on the proliferative capacity of B cells in response to IgM cross-linking (2). In addition, IL-2 and IL-4 production was lower in Bam32 knockout $CD4^+$ lymph node T cells than in wild-type cells. Although the effect on IL-2 production was somewhat variable, the effect on IL-4 production was consistent among four experiments. In general, IFNγ production was unchanged or slightly stimulated in Bam32 knockout $CD4^+$ T cells. Other cytokines that were not significantly affected by the Bam32 mutation were IL-10, IL-17 and tumor necrosis factor α (data not shown).

To investigate what signaling pathways might contribute to the defect in proliferation and IL-4 production seen in Bam32 knockout $CD4^+$ lymph node T cells, we measured TCR-induced calcium flux and TCR-induced MAPK activation in these cells. To measure TCR-induced calcium flux, lymph node cells were loaded with the ratiometric calcium-sensitive dye indo-1 and were stimulated with a range of concentrations of biotinylated anti-CD3 and anti-CD4

antibodies. The antibodies were cross-linked using streptavidin. The ratio of indo-violet to indo-blue fluorescence was measured over time. As shown in Fig. 3A, TCR-induced calcium flux was normal in Bam32 knockout $CD4^+$ lymph node T cells. This was true over a range of stimulatory antibody concentrations (data not shown). These data are consistent with the lack of effect seen on calcium flux in IgM-stimulated Bam32 knockout B cells (2). Levels of phospho-Erk, phospho-Jnk and phospho-p38 were measured by western blotting of total cellular lysates from purified $CD4^+$ lymph node T cells and are presented in Fig. 3B. Levels of phospho-protein normalized for levels of total protein are shown in the graphs in Fig. 3B. Plate-bound antibody stimulation conditions were chosen that corresponded to low levels of stimulation (2.5 μg ml^{-1} anti-CD3 for pErk and pJNK). Normalized levels of pJNK and p-p38 were similar in Bam32 knockout $CD4^+$ T cells compared with wild-type controls over 30 min of TCR stimulation. However, normalized pErk levels were consistently decreased in $CD4^+$ lymph node T cells from Bam32 knockout mice relative to control $CD4^+$ T cells. This effect was also seen using flow cytometry (Fig. 3C). This defect in Erk signaling is similar to signaling defects previously observed in Bam32 null B cells (2). Although Bam32 null B cells showed decreased Jnk activation (2), we did not observe a consistent decrease in normalized pJNK levels in Bam32 knockout $CD4^+$ lymph node T cells.

Since Bam32 transfection resulted in altered actin remodeling in human B cell lines (7), we examined the spreading ability and actin organization of Bam32 knockout $CD4^+$ lymph node T cells using an assay previously utilized in the lab to study actin-dependent T cell spreading (15). In this assay, T cells are dropped onto chambers previously coated with stimulatory antibodies and the spreading cells are monitored by confocal microscopy. Here, $CD4^+$ lymph node T cells from wild-type and Bam32 knockout mice were dropped onto stimulatory surfaces pre-coated with anti-CD3 + anti-CD28 antibodies. The T cells were fixed and stained for F-actin (phalloidin) and phospho-ZAP-70, which is associated with the TCR. Single cells and fields of cells are presented in Fig. 4. T cells from Bam32 knockout mice showed less spreading than controls (Fig. 4), while cell size was shown to be equivalent by flow cytometry for the cells in suspension before dropping onto the stimulatory cover slips (data not shown). After 15 min of spreading, the spread cell size was quantified as described in Methods. Bam32 knockout $CD4^+$ lymph node T cells showed a smaller spread cell size than controls (5.69×10^7 $nm^2 \pm 0.20 \times 10^7$ nm^2 for control cells versus 4.24×10^7 $nm^2 \pm 0.18 \times 10^7$ nm^2 for Bam32 knockout cells, Fig. 4C). As shown by phalloidin staining, well-formed rings of actin staining were more readily observed in control than in Bam32 knockout T cells. ZAP-70-containing signaling microclusters were observed in both Bam32-deficient and control T cells.

Finally, because defective BCR internalization has been reported in Bam32-deficient DT40 B cells (8), we also measured TCR internalization in $CD4^+$ T cells from wild-type and Bam32 knockout mice. As shown in Fig. 5, stimulation of lymph node T cells by plate-bound anti-CD3 resulted in down-modulation of the TCR in both wild-type and $Bam32^{-/-}$ $CD4^+$ T cells. In addition, the rate of TCR down-modulation was not significantly affected by the Bam32 null mutation.

Discussion

Our studies reveal several defects of Bam32-deficient T cells. TCR-mediated spreading, a measure of cytoskeletal function, was impaired as was TCR-mediated cellular proliferation and elaboration of several cytokines. Despite these findings, there was no observed effect on T cell development or thymocyte selection. On a molecular level, TCR-mediated Erk activation was decreased whereas TCR-induced Ca^{++} influx and activation of several other signaling molecules were not significantly affected. Although it is tempting to speculate that a defect in Erk activation results in decreased T cell proliferation based on the role of Erk in mitogenesis in other systems (18), we have no direct evidence for such a link in these T cells.

Bam32 may mediate signal transduction from the TCR to Erk activation in a previously unrecognized pathway. The requirement for intact LAT for Erk activation is well documented (19,20). Two pathways downstream of LAT that may mediate Ras/Erk activation are the classic Grb2/Sos pathway and the more recently defined PLC-γ1/RasGRP pathway (13). We previously described a mouse model that expresses a mutant form of LAT that cannot bind PLC-γ1 (21). Although TCR-induced Ca^{++} influx was dramatically reduced in T cells from these mice, Erk activation was not. One mechanism whereby Erk could be activated in these T cells is through Grb2 and Sos. However, there also remained the possibility of additional mechanisms for Erk activation in T cells. In light of its connection to Erk activation in B cells, we were led to investigate the role of Bam32 as an additional adapter protein that could mediate Erk activation in T cells.

In the context of intact TCR and LAT signaling, it was something of a surprise to observe defective Erk activation in Bam32-deficient T cells. However, Erk activation defects have been observed in the absence of Bam32 in both B and, now, T cells. The mechanism by which Bam32 is coupled to Erk is not clear. There is no evidence of Bam32 tyrosine phosphorylation in T cells and our efforts to detect Bam32 protein have not been successful due to low levels of Bam32 protein in T cells and/or inadequate antibodies (data not shown). Nonetheless, the functional effects of Bam32 are clear. Identification of this pathway now enables us to further probe the mechanisms of Erk activation in normal T cells and in the setting of LAT mutations.

Acknowledgements

The authors wish to thank Barbara J. Taylor of the National Cancer Institute Flow Cytometry Core Facility for help with sorting and Michel Nussenzweig of Rockefeller University for providing Bam32 knockout mice.

Funding

Intramural Research Program of the National Institutes of Health; National Cancer Institute; Center for Cancer Research.

Abbreviations

BCR, B cell receptor
DAG, diacylglycerol
IP3, inositol (1,4,5) tris-phosphate
IRM, interference reflection microscopic
MAPK, mitogen-activated protein kinase
MFI, mean fluorescence intensity
PH, pleckstrin homology
PI3K, phosphoinositide-3 kinase
RasGEF, Ras guanine exchange factor
RT, reverse transcription
Sos, Son of sevenless
TCR, T cell antigen receptor

References

1. Allam A, Marshall AJ. Role of the adaptor proteins Bam32, TAPP1 and TAPP2 in lymphocyte activation. Immunol. Lett 2005;97:7. [PubMed: 15626471]
2. Han A, Saijo K, Mecklenbrauker I, Tarakhovsky A, Nussenzweig MC. Bam32 links the B cell receptor to ERK and JNK and mediates B cell proliferation but not survival. Immunity 2003;19:621. [PubMed: 14563325]

3. Isakoff SJ, Cardozo T, Andreev J, et al. Identification and analysis of PH domain-containing targets of phosphatidylinositol 3-kinase using a novel *in vivo* assay in yeast. EMBO J 1998;17:5374. [PubMed: 9736615]
4. Dowler S, Currie RA, Downes CP, Alessi DR. DAPP1: a dual adaptor for phosphotyrosine and 3-phosphoinositides. Biochem. J 1999;342(Pt 1):7. [PubMed: 10432293]
5. Rao VR, Corradetti MN, Chen J, et al. Expression cloning of protein targets for 3-phosphorylated phosphoinositides. J. Biol. Chem 1999;274:37893. [PubMed: 10608855]
6. Marshall AJ, Niiro H, Lerner CG, et al. A novel B lymphocyte-associated adaptor protein, Bam32, regulates antigen receptor signaling downstream of phosphatidylinositol 3-kinase. J. Exp. Med 2000;191:1319. [PubMed: 10770799]
7. Allam A, Niiro H, Clark EA, Marshall AJ. The adaptor protein Bam32 regulates Rac1 activation and actin remodeling through a phosphorylation-dependent mechanism. J. Biol. Chem 2004;279:39775. [PubMed: 15247305]
8. Niiro H, Allam A, Stoddart A, Brodsky FM, Marshall AJ, Clark EA. The B lymphocyte adaptor molecule of 32 kilodaltons (Bam32) regulates B cell antigen receptor internalization. J. Immunol 2004;173:5601. [PubMed: 15494510]
9. Fournier E, Isakoff SJ, Ko K, et al. The B cell SH2/PH domain-containing adaptor Bam32/DAPP1 is required for T cell-independent II antigen responses. Curr. Biol 2003;13:1858. [PubMed: 14588241]
10. Wange RL. LAT, the linker for activation of T cells: a bridge between T cell-specific and general signaling pathways. Sci. STKE 2000;2000:RE1. [PubMed: 11752630]
11. Sommers CL, Samelson LE, Love PE. LAT: a T lymphocyte adapter protein that couples the antigen receptor to downstream signaling pathways. Bioessays 2004;26:61. [PubMed: 14696041]
12. Mor A, Philips MR. Compartmentalized Ras/MAPK signaling. Annu. Rev. Immunol 2006;24:771. [PubMed: 16551266]
13. Genot E, Cantrell DA. Ras regulation and function in lymphocytes. Curr. Opin. Immunol 2000;12:289. [PubMed: 10781411]
14. Sommers CL, Rabin RL, Grinberg A, Tsay HC, Farber J, Love PE. A role for the Tec family tyrosine kinase Txk in T cell activation and thymocyte selection. J. Exp. Med 1999;190:1427. [PubMed: 10562318]
15. Barda-Saad M, Braiman A, Titerence R, Bunnell SC, Barr VA, Samelson LE. Dynamic molecular interactions linking the T cell antigen receptor to the actin cytoskeleton. Nat. Immunol 2005;6:80. [PubMed: 15558067]
16. Sommers CL, Lee J, Steiner KL, et al. Mutation of the phospholipase C-gamma1-binding site of LAT affects both positive and negative thymocyte selection. J. Exp. Med 2005;201:1125. [PubMed: 15795236]
17. Azzam HS, DeJarnette JB, Huang K, et al. Fine tuning of TCR signaling by CD5. J. Immunol 2001;166:5464. [PubMed: 11313384]
18. Meloche S, Pouyssegur J. The ERK1/2 mitogen-activated protein kinase pathway as a master regulator of the G1-to S-transition. Oncogene 2007;26:3227. [PubMed: 17496918]
19. Zhang W, Trible RP, Zhu M, Liu SK, McGlade CJ, Samelson LE. Association of Grb2, Gads, and phospholipase C-gamma 1 with phosphorylated LAT tyrosine residues. Effect of LAT tyrosine mutations on T cell antigen receptor-mediated signaling. J. Biol. Chem 2000;275:23355. [PubMed: 10811803]
20. Lin J, Weiss A. Identification of the minimal tyrosine residues required for linker for activation of T cell function. J. Biol. Chem 2001;276:29588. [PubMed: 11395491]
21. Sommers CL, Park CS, Lee J, et al. A LAT mutation that inhibits T cell development yet induces lymphoproliferation. Science 2002;296:2040. [PubMed: 12065840]

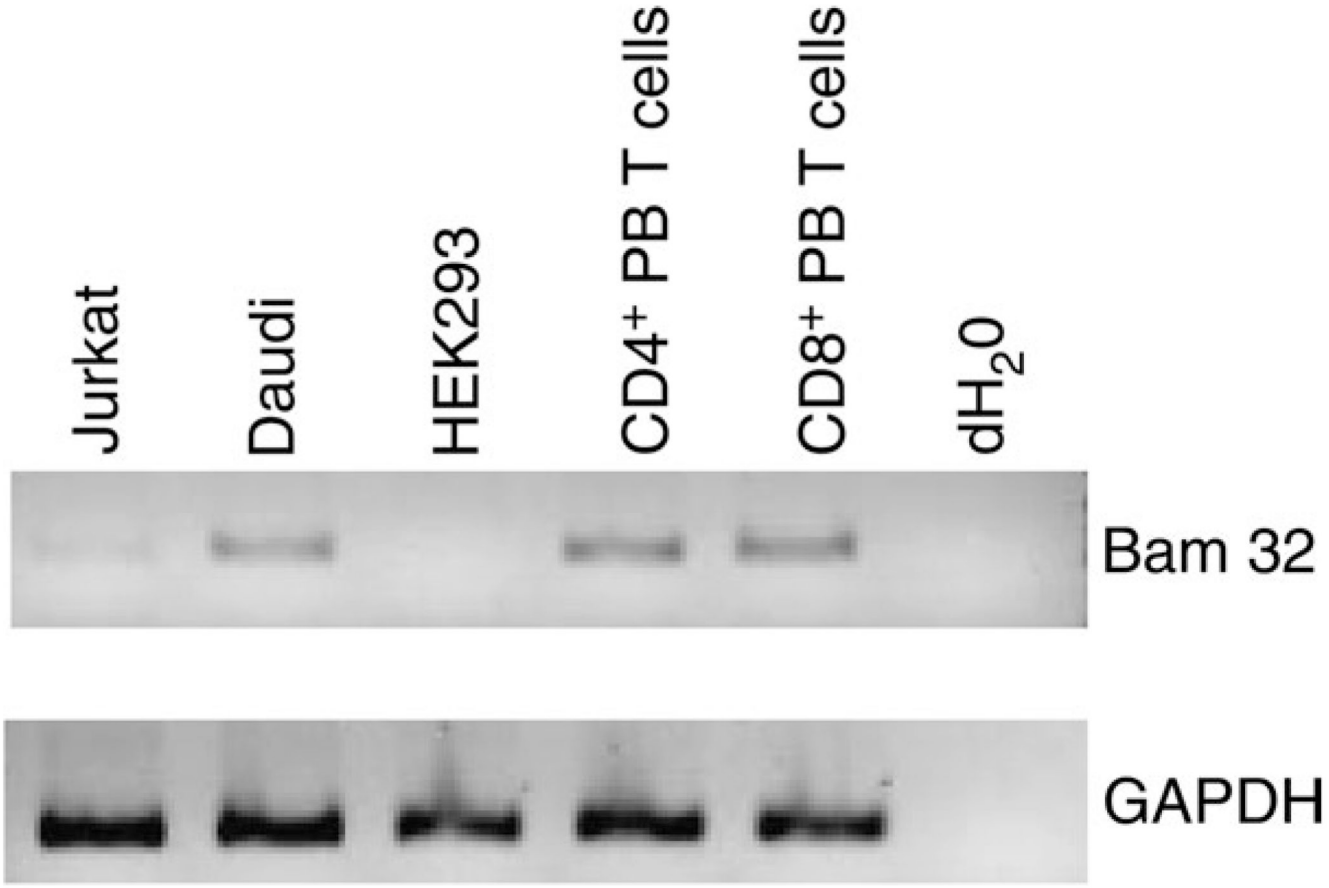

Fig. 1.

Bam32 expression in human cell lines and human peripheral T cells. RNA was extracted from the following cell lines: Jurkat (origin—T cell leukemia), Daudi (origin—Burkitt's lymphoma) and HEK293 (origin—kidney epithelium) or from sorted human peripheral blood (PB) T cells. After RT, cDNA was analyzed by PCR for expression of Bam32 and GAPDH.

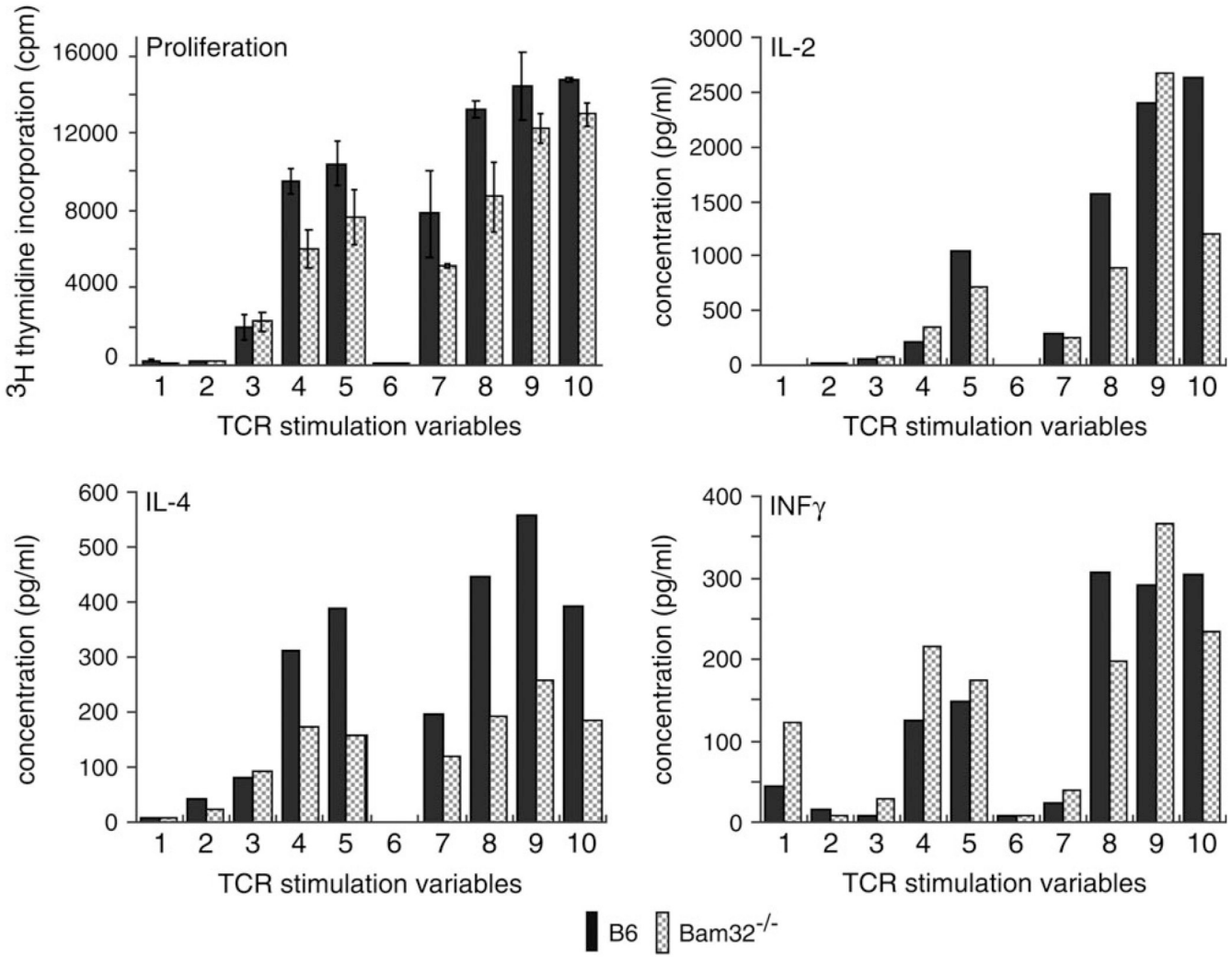

Fig. 2.

Bam32 contribution to proliferation and cytokine production in CD4$^+$ T cells. CD4$^+$ T cells were purified from lymph node cells from 8– to 11-week-old C57BL/6 (B6) and Bam32$^{-/-}$ mice (>90% purity). Cells were then plated in wells pre-coated with the following concentrations of anti-CD3 and anti-CD28: (1) PBS control, (2) 1 μg ml^{-1} anti-CD3, (3) 2.5 μg ml^{-1} anti-CD3, (4) 5 μg ml^{-1} anti-CD3, (5) 10 μg ml^{-1} anti-CD3, (6) 5 μg ml^{-1} anti-CD28, (7) 1 μgml^{-1} anti-CD3 + 5 μgml^{-1} anti-CD28, (8) 2.5 μgml^{-1} anti-CD3 + 5 μgml^{-1} anti-CD28, (9) 5 μgml^{-1} anti-CD3 + 5 μgml^{-1} anti-CD28 and (10) 10 μg ml^{-1} anti-CD3 + 5 μg ml^{-1} anti-CD28. After 48 h incubation, proliferation was measured by ^{3}H-thymidine incorporation. Cytokine production was quantified by SearchLight protein array analysis of culture supernatants. Triplicate wells were analyzed individually for proliferation and culture supernatants were pooled for cytokine analysis. Results are representative of four experiments.

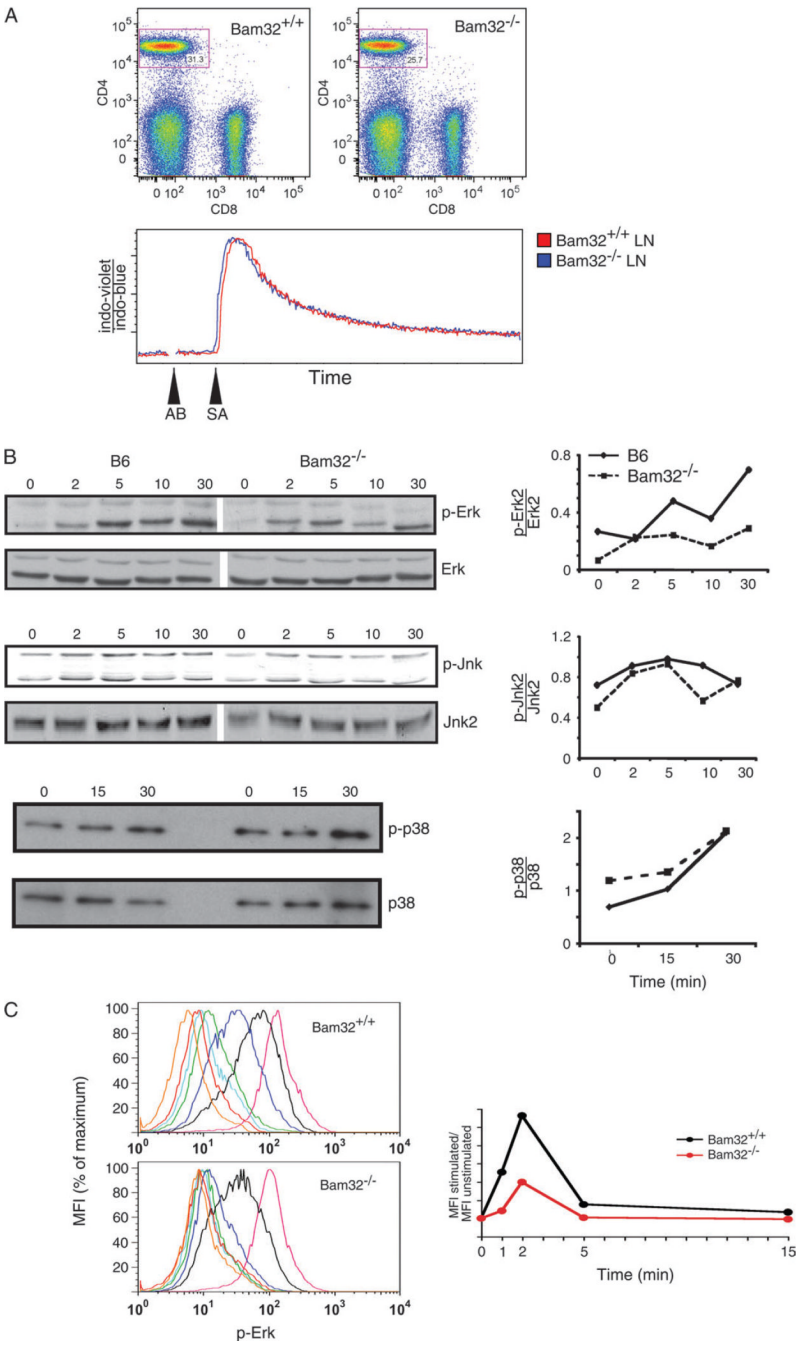

Fig. 3.

Signal transduction in Bam32$^{-/-}$ CD4^{+} T cells. (A) TCR-induced calcium flux in Bam32$^{-/-}$ CD4^{+} T cells. Lymph node cells from 11-week-old Bam32$^{+/+}$ and Bam32$^{-/-}$ littermates were loaded with indo-1 and surface stained for CD4 and CD8. Biotinylated anti-CD3 (0.5 μg ml^{-1}) and anti-CD4 (10 μg ml^{-1}) were added at 30 s and streptavidin (80 μg ml^{-1}) at 60 s (represented by AB and SA arrowheads). CD4 CD8 dot plots are shown and calcium kinetic data are shown for gated CD4^{+} cells over 6 min. (B) TCR-induced Erk, Jnk and p38 MAPK activation in Bam32$^{-/-}$ CD4^{+} T cells. CD4^{+} T cells were purified from lymph nodes of C57BL/6 (B6) and Bam32$^{-/-}$ mice (8 weeks) by negative magnetic bead separation. For Erk and Jnk analyses, CD4^{+} T cells were then stimulated using 2.5 μg ml^{-1} plate-bound anti-CD3 for the

indicated periods of time (minutes). For p38 analysis, rested cells were stimulated with 5 μg ml^{-1} plate-bound anti-CD3 + 5 μg ml^{-1} anti-CD28. Total cell lysates were then analyzed by western blotting for the indicated proteins or phospho-proteins. Graphs show the ratio of the levels of phospho-protein to total protein as determined by densitometry. Data are representative of at least three experiments. (C) Lymph node cells from 7– to 8-week-old $Bam32^{+/+}$ and $Bam32^{-/-}$ mice were stimulated with anti-CD3 + anti-CD4 in solution, fixed, permeabilized, stained and analyzed by flow cytometry. Histograms are shown for gated $CD4^{+}$ lymph node cells. Stimulation conditions were as follows: red line, no stimulation; dark blue line, 1 min stimulation; black line, 2 min stimulation; green line, 5 min stimulation; light blue line, 15 min stimulation and magenta line, phorbol myristate acetate stimulation. Orange line indicates staining with a negative control antibody. On the right, mean fluorescence intensity (MFI) of antibody-stimulated versus unstimulated cells is graphed over time.

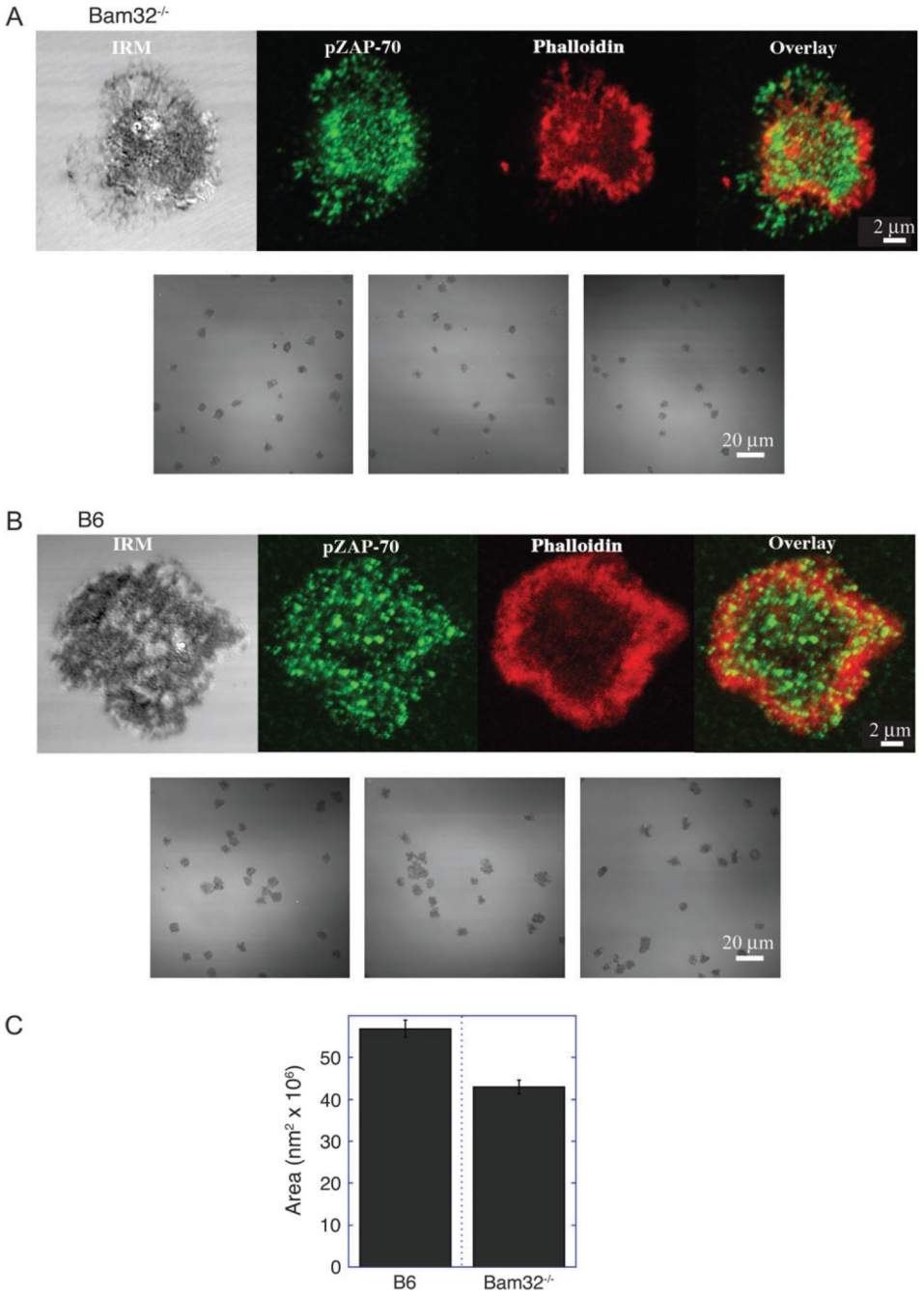

Fig. 4.

TCR-mediated spreading of$Bam32^{-/-}$ $CD4^+$ Tcells. $CD4^+$ Tcells were purified from lymph nodes of 8– to 11-week-old $Bam32^{-/-}$ (A) and C57BL/6 (B) mice by negative magnetic bead selection (>95% purity). Tcells were dropped onto chamber surfaces pre-coated with anti-CD3 (10 $\mu g ml^{-1}$) and anti-CD28 (10 $\mu g\ ml^{-1}$). After 15 min, cells were fixed and stained with phalloidin and anti-phospho-ZAP-70. Interference reflection microscopic (IRM) and confocal fluorescent images were acquired using a 63× objective with or without optical zoom (upper and lower images, respectively) and the area of spread cells was quantitated. (C) The mean and standard error of the mean of the areas are presented for C57BL/6 (n = 95 cells) and

Bam32$^{-/-}$ (n = 71 cells). Using a Student's t-test for unpaired data with unequal variance, the two means differ at a probability value of <0.0001.

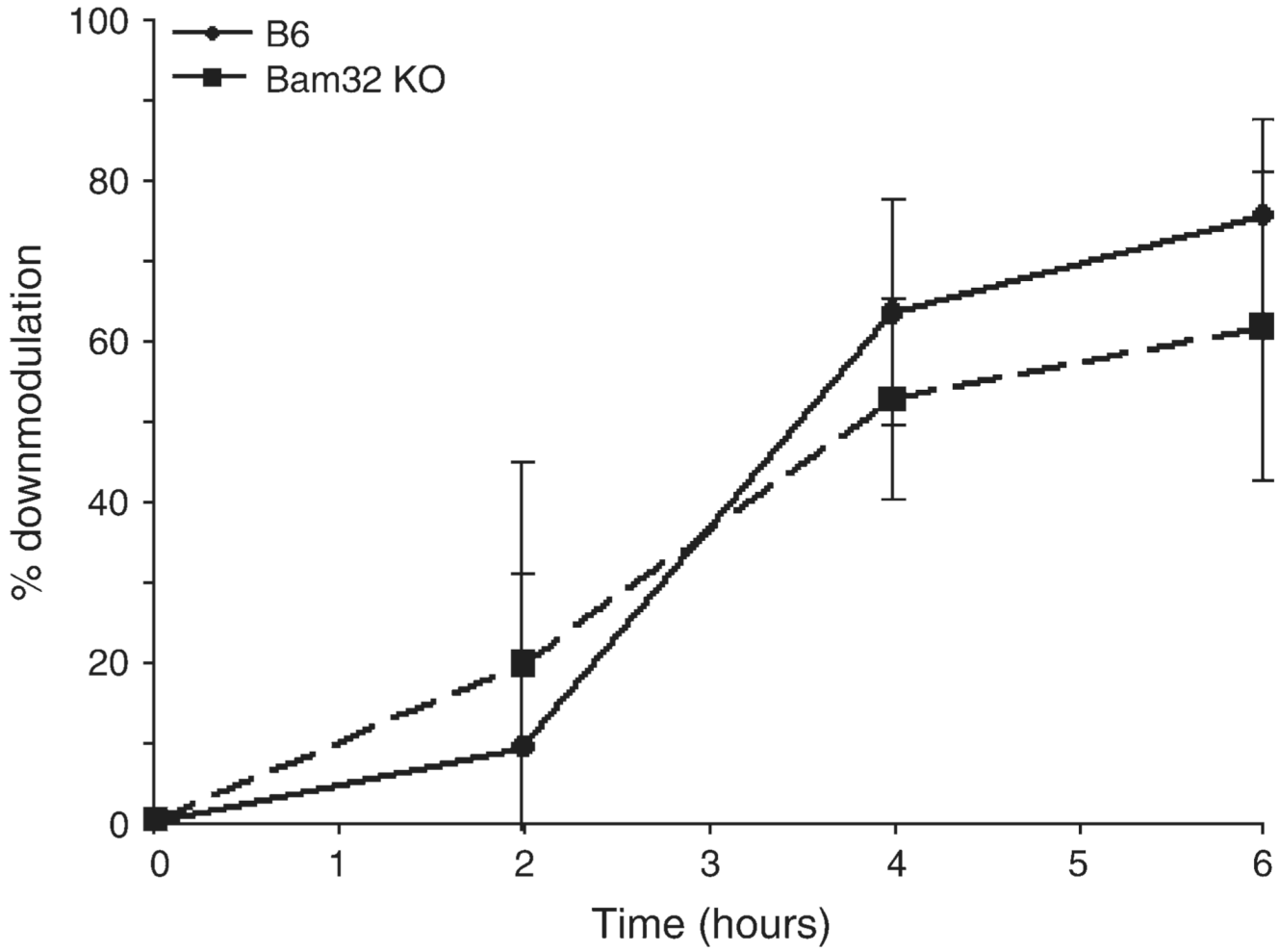

Fig. 5.

TCR down-modulation in Bam32$^{-/-}$ CD4^{+} T cells. Lymph node T cells from C57BL/6 (B6) and Bam32$^{-/-}$ mice were stimulated with plate-bound anti-CD3 for the number of hours indicated. Surface TCRβ was quantitated by flow cytometry and % down-modulation calculated as described in Methods